신장 광 레오미터와 소각 X선 산란 방법을 이용한 신장 유동계 내의 삼성분 블록 공중합체의 모폴로지 변화 연구

권용구, Yuka Kobori*, Masami Okamoto*, Tadao Kotaka*

인하대학교 고분자 공학과, *Toyota Technological Institute

Elongational Flow-Induced Morphological Change of Triblock Copolymer Melt: Elongational Flow-Opto Rheometry and Small Angle X-ray Scattering Study

Yong Ku Kwon, Yuka Kobori*, Masami Okamoto*, Tadao Kotaka*

Department of Polymer Science and Engineering, Inha University, Inchon 402-751, Korea, *Advanced Polymeric Materials Engineering, Toyota Technological Institute, Hisakata 2-12-1, Tempaku, Nagoya 468-8511, Japan

Introduction

The elongational flow behavior of heterogeneous polymer melts such as block copolymers and polymer blends is complicated due to the structural evolution of phase morphology, as well as the nonlinear elongational flow-response of the component polymers [1-5]. Nanophase-separated block copolymers are known to display phase morphologies which vary with the chemistry and composition of each block segment [6]. Deformation behavior of block copolymers in a laminar shear flow field has been widely investigated in great details. It has been reported that a large amplitude oscillating shear applied on diblock copolymers induces the alignment of domains into either the parallel or perpendicular orientation, depending on the shearing temperature and molecular weight of the individual blocks.

Elongational deformation of block copolymers has attracted recent research interests due to their interesting morphological responses on elongation [4]. Most of studies reported have been carried out below the T_g of the rigid component block, which results in the deformation at small strains and in localized regions or at defects. Our previous study, carried out at high temperatures between the T_g of the rigid block and the order-disorder transition (ODT) of the block copolymers, also pointed out that the elongated morphology of the cylindrical and spherical microdomains was controlled by the applied strain rate, where the fast elongation resulted in a tilted phase, whereas the slow elongation generated the parallel alignment of the cylindrical phase [5]. The elongational viscosity, $\eta_E(\dot{\varepsilon}_0;t)$ was extremely increased with low stain rates (strain-induced hardening), indicating that both molecules and domains were highly oriented to the stretching direction.

In thisstudy, we continue to investigate the elongational deformation behavior of the cylindrical morphology of SEBS triblock copolymer by using elongational flow opto-rheometry (EFOR) and small angle X-ray scattering (SAXS). This study attempts to provide the detailed explanation on the structural and morphological evolution of the cylindrical phase in the elongational-flow field and to describe the molecular features at various stages of elongation. The EFOR measurements in this study were performed at high temperature between the T_g of the polystyrene (PS) block and the reported ODT of SEBS, which seemed advantageous for monitoring the molecular and domain deformation during

elongation.

Experimental Section

1. Materials and Sample Preparation

The SEBS triblock copolymer with PS weight fraction of 30 % (*Asahi Chemical Co.*) was used in this study. The molecular weight of the polymer was determined by gel permeation chromatography (GPC) using PS elution standards: a weight-average molecular weight, M_w was 92.6 kg mol^{-1} and a polydispersity index, M_w/M_n was around 1.17. The ODT of SEBS could not be detected up to ~300 °C in our rheological measurement and has been estimated to be greater than 300 °C. The block sequence of the polymer was estimated to be 13.9-64.8-13.9 in the unit of kg mol^{-1}. The compressed films of as-received SEBS pellets were prepared by molding at 200 °C. The alignment of the cylinder domains was achieved by uniaxial roll processing by counterrotating two rollers at 200 °C for about 10 min. Then it was subsequently transferred to another hot-press kept at ambient temperature and pressure without applying load and allowed to be cooled by circulating chilled water into the jacket of the hot-press. Specimens for the EFOR measurements with dimensions of about 60.0 ± 0.8 (length) × 7.0 ± 0.4 (width) × 2.5 ± 0.5 (thickness) mm^3 were prepared by cutting the roll-cast sheet in the direction either parallel (denotes case I) or perpendicular (case II) to the rolling direction.

2. SAXS Apparatus

The measurements were carried out in our SAXS apparatus consisting of a 6 kW rotating-anode X-ray generator ($M06X^{CE}$, MAC science Co. Ltd., Ishikawa, Japan) with CuKα radiation (wavelength, λ_{scat} = 0.154 nm), operated at 50 kV and 24 mA. The distance between the sample and detector was set by 700 mm. The correction for slit-width smearing was not needed due to the fine cross-section (0.1 mm × 1 mm) of the primary X-ray beam used in this study.

3. EFOR Measurement

The elongational flow opto-rheometer employed in our study is a combination of a Meissner's new elongational rheometer of gas-cushion type commercialized as Rheometrics Melt Elongational Rheometer (RME: *Rheometrics Scientific Co.*) which has been described elsewhere [7]. In our measurement, a sample strip was clamped between two metal belt conveyers at a fixed distance L_o and annealed at 180 °C for 120 sec to remove mechanical and thermal history on samples acquired prior to elongation. The EFOR measurements in this study were carried out with a strain rate, 0.01 s^{-1} at 180°C. The tensile force and retardation were directly measured during the EFOR measurement. Assuming no volume change during elongation, both cross-sectional area and thickness can be estimated from the initial dimensions measured prior to elongation.

Results and Discussion

Figures 1 (a) and (b) show elongational viscosities, $\eta_E(\dot{\varepsilon}_0;t)$s of the case I and II sample, elongated with a strain rate of 0.01 s^{-1} at 180 °C. The data showed that the $\eta_E(\dot{\varepsilon}_0;t)$ of the case I sample increased continuously with time up to near ε = 0.4, followed by a decrease to almost the steady state before rupture, whereas that of the case II sample

exhibited the complicated behavior during elongation. The points where the $\eta_E(\dot{\varepsilon}_0;t)$ began to decrease were related with the strain-induced softening behavior, as described in our previous papers [5]. In Fig. 1 (a), the data did not show any solid plateau region, where $\eta_E(\dot{\varepsilon}_0;t)$ was independent of $\dot{\varepsilon}_0$, revealing that the steady state during elongation was almost absent. Due to the parallel arrangement of the PS and PEB domains, the initial elongation of the case I sample may cause the realignment of the PS and PEB domains to the stretching direction, which exhibits the initial increase of the $\eta_E(\dot{\varepsilon}_0;t)$ up to $\varepsilon = 0.4$. The further elongation above this point may lead to the deformation of the domain and grain structure which decreases the value of the $\eta_E(\dot{\varepsilon}_0;t)$ to almost the steady state before rupture.

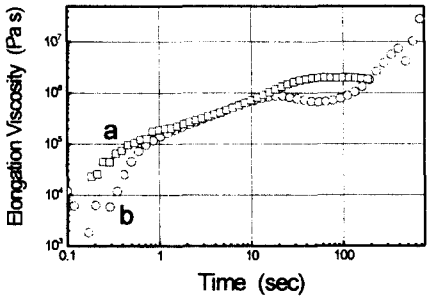

Fig. 1. Elongational viscosities of the case I and II melts

The change of the $\eta_E(\dot{\varepsilon}_0;t)$ of the case II sample can be divided by three regions with elongation time: an initial increase up to $\varepsilon = 0.2$; a following decrease to almost the steady state in the range of $0.2 < \varepsilon \leq 0.7$; a relatively rapid final increase before rupture. Due to the alternative arrangement of the PS and PEB domains to the stretching direction, the initial increase of the $\eta_E(\dot{\varepsilon}_0;t)$ of the case II sample was caused by the reorientation of the PEB matrix which was preferentially deformed in the beginning. On further elongation, yielding of the cylinder structure was occurred along the stretching direction, leading to the deformation and rotation of the cylinder phase in the middle of elongation. In the final stage of elongation, the further elongation of the yield state of the case II sample caused the reorganization or realignment of the yielded cylinder domains, exhibiting the final increase of the $\eta_E(\dot{\varepsilon}_0;t)$, indicative of the strain-induced hardening behavior.

Figures 2 (a) through (e) showed the SAXS data of the unelongated and elongated case II sample collected at: (a) 0 sec (unoriented); (b) 20 sec ($\varepsilon = 0.2$, $\lambda = 1.2$); (c) 70 sec ($\varepsilon = 0.7$, $\lambda = 1.9$); (d) 200 sec ($\varepsilon = 2$, $\lambda = 7.4$); (e) 400 sec ($\varepsilon = 4$, $\lambda = 54.6$). The corresponding one-dimensional meridional SAXS intensities $I(q)$ *vs* the scattering vector, q, were also shown in Figs 2 (a) through (e). Fig. 2 (a) exhibited a series of the SAXS peak intensities in the meridional direction, the same as the stretching direction, confirmed that the initial cylinders before elongation were aligned perpendicular to the stretching direction. The most strong peaks corresponded to the hexagonal *100* peak and the additional X-ray intensities were higher order hexagonal peaks whose the q values were almost in the ratio of $1:\sqrt{3}:\sqrt{7}$. The existence of the meridional peak intensities of the initial case II sample

indicated the alignment of the two-dimensional lattice in the direction perpendicular to the stretching direction. Based on the position of the most intense *100* reflection, the cylinder diameters, *D*s, of the elongated case II samples were estimated. The slight increase of the diameters at $\varepsilon = 0.2$ and 0.7 was due to the increased structural imperfection of the cylinder phase, generated by the deformation and rotation of the initial cylinder morphology. Hereafter, the diameter was then slightly decreased again by the improved molecular and domain orientation to the stretching direction.

(a) (b) (c) (d) (e)

Figure 2: SAXS data of the unelongated and elongated case II samples

Conclusions

The combination of the EFOR and SAXS measurements provided the information on the structural evolution of the cylindrical domains under elongation. The deformation behavior varied with the initial alignment of the cylinder domains. The elongation of the case I sample induced the preferential elongation of the relatively rigid PS domains in the beginning of elongation and the initial parallel morphology was almost persisted at large deformation up to rupture. The reorganization of the grain structure, along with yielding of the PS domains decreased the $\eta_E(\dot{\varepsilon}_0;t)$ beyond the yielding point of the case I sample. For the case II sample, the initial elongation induced the elongation of the soft PEB matrix. The continuous elongation of the case II sample deformed and rotated the initial grain structure to the stretching direction. The deformation of the grain and domain structure decreased the $\eta_E(\dot{\varepsilon}_0;t)$ values in the range of $0.2 < \varepsilon \leq 0.7$, but the further orientation of the molecules and cylinders at high degree of elongation highly increased the $\eta_E(\dot{\varepsilon}_0;t)$ and exhibited the prominent strain-induced hardening behavior. The changes of $\eta_E(\dot{\varepsilon}_0;t)$s of the case I and II samples were mostly governed by the morphological evolution of the cylinder domain and grain structures of both samples.

References

[1] M. Okamoto, A. Kojima, T. Kotaka, *Polymer,* **39**, 2149 (1997).

[2] Y. Kano, M. Okamoto, T. Kotaka, *Polymer,* **40**, 2459 (1999).

[3] Y. H. Kim, M. Okamoto, T. Kotaka, T. Ougizawa, T. Tchiba, T. Inoue, *Polymer,* **41**, 4747 (2000).

[4] T. Takahashi, H. Toda, K. Minagawa, J.-I. Takimoto, K. Iwakura, K. Koyama, *J. Appl. Polym. Sci.,* **56**, 411, (1995).

[5] T. Kotaka, M. Okamoto, A. Kojima, Y. K. Kwon, S. Nojima, *Polymer*, accepted for publication; T. Kotaka, M. Okamoto, A. Kojima, Y. K. Kwon, S. Nojima, *Polymer*, accepted for publication.

[6] I. W. Hamley, Melt Phase Behaviour of Block Copolymers. In *The Physics of Block Copolymers*: Oxford University Press, Inc., New York, 1998.

[7] T. Kotaka, A. Kojima, M. Okamoto, *Rheol. Acta,* **36**, 646 (1997).